

# Characteristic Analysis and Design of a Single Phase Switched Reluctance Motor for High Speed Application

Youn-Hyun Kim<sup>†</sup>

**Abstract** - Switched reluctance motors have received much attention as a driving means for various industrial applications because they have simple construction, low cost and high efficiency. Nevertheless, the requirements of drive converters make it difficult to lower the overall system cost as compared with the DC motor application. Single phase switched reluctance motors (SPSRMs) provide a solution to the high cost problem since the number of switching power devices can be reduced and consequently the trials for application are increased. However, research involving SPSRMs, especially in the area of design work, is insufficient. This paper introduces a novel design methodology of single phase SRM. The design work for SPSRM comprises the determination of many variables such as stator and rotor pole arc as well as on, off and so on. Managing all variable combinations leads to lengthy computation time and a fault in the design process. For that reason, a reliable technique and brief procedure term are required in SPSRM design.

**Keywords:** High speed application, Motor design methodology, Pole arc, Single Phase Switched Reluctance Motors

## 1. Introduction

The SRM (Switched Reluctance Motor) is an electric machine that consists of a simple structure with a winding only on the stator and not on the rotor. In other words, there are no windings, conductors or any permanent magnets on the rotor. The costs are lower than other motors due to its simple construction. It is easy to implement a high speed drive system and both the torque and efficiency of the unit volume are highly superior to all others. Therefore, the SRM is thought to be a valuable replacement for conventional type motors in various industry applications [1-3]. Although the cost for manufacturing the motor may be competitive, the overall cost of the system including the power converter is not low. This has limited the applications of the SRM to only those areas that require variable speed drives in home appliances. To reduce the cost of the drive system, the applications of the single phase SRM, which can reduce the number of required devices of switching devices, is now being focused on [4-6].

The motor design is usually divided into two steps. One is a basic design such as the electric and magnetic loading distribution method and another is an advanced design with a detailed design procedure that uses FEM (Finite Element Method) for analysis. Since the basic design method mostly depends on the experiences of design, it is not easy

to design new types of motors. Moreover, the SRMs are generally driven in the nonlinear region, which means that designs based only on the mathematical calculations of formulas can cause errors. This brings a necessity for using numerical analysis such as FEM to consider the nonlinearity of the magnetic fields. However, using the advanced design method requires a great deal of time for simulation and particularly for the SRM. Since we have to consider the turn-on angle, the process takes a much longer time. Although the basic theories were proposed in the 1980s by Lawrenson, we still need a detailed and well organized design method for the SRM and especially for a single phase configuration [7].

Therefore, this paper presents an innovative approach for the design strategy of a single phase SRM for high speed applications using the single phase SRM. The drive factors, such as angles of rotor and stator, turn-on and turn-off angle, are also considered in the proposed design method.

## 2. Design Strategy for Single Phase SRM

### 2.1 Specifications of the motor

Fig. 1 shows the cross section of the basic analysis model, the single phase 6/6 SRM. The motor is configured to have 3 poles. The path of the magnetic flux is made to be as short as possible in order to reduce the magnetic resistance. Each of the windings is connected in parallel fashion.

<sup>†</sup> Corresponding Author: Dept. of Electrical and Electronic Engineering, Hanbat University, Korea. (yhyunk@hanbat.ac.kr)

This paper is focused on the application of the motor for a vacuum cleaner. The output power is 540[W] and the efficiency is 60% while the rated output of the motor is 900[W]. To lower the cost, a capacitor with low capacitance is placed at the DC link of the converter. Due to the low capacitance, the voltage across the DC link can be assumed to be a fully rectified waveform of a conventional AC 220[V] sinusoidal source, instead of a smoothly regulated voltage. Thus, the value of the input voltage to the motor is 190[V], which is the average value of the fully rectified voltage of AC 220[V]. The rated speed is 35,000[rpm] and other specifications are shown in Table 1.

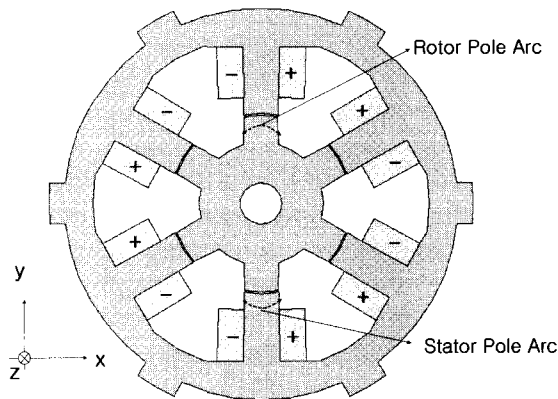


Fig. 1 The cross section of the basic analysis model

Table 1 The specifications of the basic design model

|               |             |                 |          |
|---------------|-------------|-----------------|----------|
| Rated Power   | 900 [W]     | Rotor Diameter  | 35 [mm]  |
| Rated Voltage | 190 [V]     | Stator Yoke     | 6 [mm]   |
| Speed         | 35,000[rpm] | Rotor Yoke      | 6 [mm]   |
| Phase         | 1           | Stator Diameter | 80 [mm]  |
| Stator Pole   | 6           | Air Gap         | 0.3 [mm] |
| Rotor Pole    | 6           | Stack Length    | 33 [mm]  |
| Core          | S18         | Coil Part Ratio | 10 [%]   |

## 2.2 Procedure of the design of single phase SRM

To satisfy both the power conditions of the application and the required performance from a given volume, not only the mechanical variables such as the shape of the rotor and stator but also the electrical variables, for example, the turn-on and turn-off angle should be considered. Subsequently, there are many choices of design variable combinations and also, due to the nonlinearity of the magnetic field, the performance test should be evaluated by numerical analysis because of the nonlinearity of the magnetic field such as FEM (Finite Element Analysis). Furthermore, for a reliable investigative result of the design, the transient tests using a voltage source should be used. Since it takes a great deal of time and effort to derive an optimal design result, this disadvantage acts as an obstacle for designing a new type of SRM for a novel application. It

is necessary for developing a more reasonable design procedure and method that reduces the number of possible combinations of the design factors.

Usually when a motor is designed, a decision is made as to whether the design method is demonstrating a reasonable design procedure for an output torque at a rated speed. In other words, even though the sufficient flow of current can guarantee that the required amount of torque will be produced, if the back EMF generated at the required speed of the motor is greater than the voltage supplied, there would be an inadequate current flow resulting in insufficient torque. This signifies that the requirements of the motor are not satisfied. Thus, deciding the optimal value of current that can satisfy both the torque and speed requirements is very important. Unfortunately, this is very difficult and determining the starting point of the design able to satisfy the requirements is even more complicated.

Typically, when a motor is designed the main factors of design that satisfy the required output are selected. The conventional method for designing a motor is by selecting the ratio of the current to the magnetic flux. Where, the current stands for the electric load while the flux stands for the magnetic load. However, because this ratio is not determined by theoretical equations, but by the designer's experiences it is difficult to apply it to new types of motors such as the SRM. Thus, this paper proposes a design factor as the load ratio for the design of the SPSRM. This initial design factor can be selected from (1) and (2), which represents the torque and motional EMF of the SRM.

$$T = \frac{1}{2} i^2 \frac{dL}{d\theta} \quad (1)$$

$$E = i \frac{dL}{d\theta} \omega \quad (2)$$

From (1) and (2) the current and  $dL/d\theta$  that satisfy the required torque and speed are calculated. This paper proposes to choose current and  $dL/d\theta$  as an initial design factor and to decide the specifications of the coil, and the shape of the arc of both the rotor and the stator in conjunction with the number of turns, as a design method. The analysis of the  $dL/d\theta$  was performed by using FE analysis, and the increasing and decreasing time of the current were also examined by using the minimum and maximum value of the inductance. Among the models that satisfy the  $dL/d\theta$  value, the ones that have a high efficiency and a large area to generate a sufficient amount of positive torque are selected with the number of windings for each of the models. The optimal model is chosen by comparing the analysis results in detail with a changing turn-off and turn-on angle. Fig. 2 shows the design flow of the suggested method.

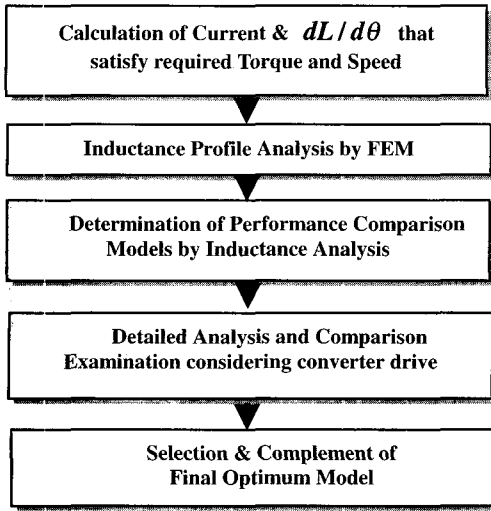


Fig. 2 The design flow of SPSRM

### 3. Design Flow of Single Phase SRM

#### 3.1 Analysis of $dL/d\theta$

Before deciding the initial design factors, current and  $dL/d\theta$ , the profile of the inductance and the characteristics of the drive should be analyzed first. The profile of the inductance and the waveform of both the torque and current for the single phase SRM 6/6 model are shown in Fig. 3. The SPSRM 6/6 model has a period of 60 degrees and the torque generated in the minimum inductance region and the maximum inductance region is slight. Most of the positive torque is generated when the inductance increases while the negative torque generates when the inductance decreases. At the minimum inductance region, it is turned on for sufficient current and it is turned off before the maximum inductance region to prevent the effect occurring due to the reverse torque generated during the inductance decreasing region. The region of the minimum inductance, increasing inductance and the maximum inductance are changed by the pole arc of the rotor and stator with a relationship as in (3), (4) and (5).

Minimum Inductance Region (A region):

$$30^\circ - (\beta_S + \beta_R) / 2 \quad (3)$$

Increment Inductance Region (B region):

$$\text{The smaller pole arc of } \beta_S, \beta_R \quad (4)$$

Maximum Inductance Region (C region):

$$(\beta_S + \beta_R) / 2 \quad (5)$$

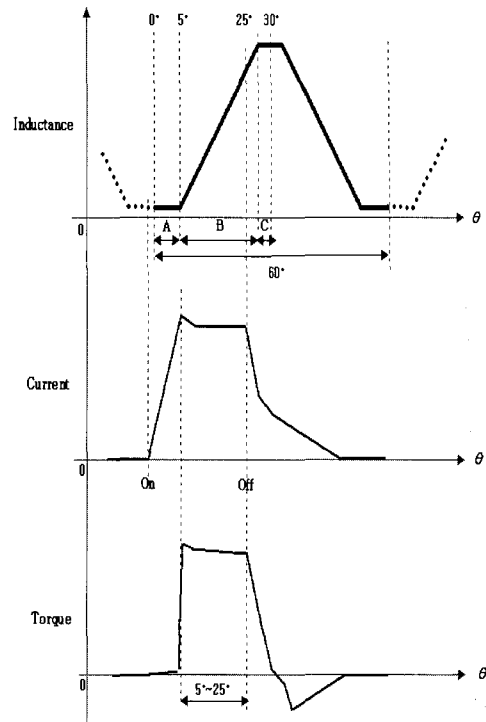


Fig. 3 Inductance, current and torque waveform of SPSRM

In this paper, the analysis of the  $dL/d\theta$  is carried out by the waveform of Fig. 3. The specification of the SPSRM is written in Chapter 2.1, the output is 900W, the DC voltage of the motor input is 190V and the rated output speed is 35,000[rpm]. The rated output torque can be calculated as 0.246N-m. However, the rated torque is defined as the average torque of a given period. As it is shown in Fig. 3, the generated torque of a SPSRM is composed of 3 regions, a positive torque region, a negative region and a region in which no torque is generated. The positive torque that is generated during the inductance increases should be larger than the average torque. If we assume that the positive and negative torque generated except between 5 to 25 degrees are cancelled out, the required torque is the torque generated for the 20 degrees, from 5 degrees to 25 degrees, and as this is one third of the period, which is 60 degrees, the torque generated could be set as three times larger than the rated torque. At this region, the  $dL/d\theta$  can be calculated as the difference of the average inductance between 5 degrees to 25 degrees. However, as the torque used in (1) is for one pole, 0.246 is substituted for the torque. According to (1) and (2) the current of a pole is 9.92[A] and the  $dL/d\theta$  is 0.005. The motional EMF is selected to be 182V considering the voltage drop across the resistor and the switch-on voltage drop of the switching device.

The analysis procedure of the  $dL/d\theta$  value is as follows. The  $dL/d\theta$  values of each of the pole arcs are calculated by using FE analysis considering the nonlinearity of the magnetic field, for the condition of a 9.92[A] current with 37 turns of the coil. As indicated in Fig. 3, the values

between 5 and 25 degrees are so reasonable that the average of this area was selected. Fig. 4 shows the contour graph of the  $dL/d\theta$  values for each of the pole arcs and the exact values of  $dL/d\theta$  are shown in Table 2.

### 3.2 Determination of performance comparison models

According to Fig. 3, the value of  $dL/d\theta$  is above 0.005, which is the required value in this paper, when the pole arc of the stator is larger than 22 degrees. In particular, the value reaches the maximum value when the pole arc is as  $(\beta_s, \beta_R = 24, 24)$  and the value is generally close to the required value 0.005 when the pole arc is as  $(\beta_s, \beta_R = 22, 22)$ . As presented in Fig. 4, there are multiple combinations for the possible pairs of the stator and rotor pole arc that satisfy the required value 0.005 as shown in Fig. 4 and also by changing the number of turns there can be more possible combinations. Thus, the pole arc combinations will be divided into 3 groups and by predicting the characteristics of each choice, the number of the possible choices will be narrowed. The first type is a group in which the pole arc of the stator and rotor are the same while the other two are groups that have different pole arcs. The second type is for the combinations occurring when the stator pole arc is larger compared to the rotor pole arc and the third is vice versa. Consequently the characteristics of the three types should be predicted by the inductance profiles of Fig. 3. Through an inspection, type 1 would be the better choice for considering the performance. There are several reasons that support this prediction. First, there is no maximum inductance region that generates small torque, and because it has a small inductance compared to the models that have a large stator arc, the rising time of the current is short, which enhances the torque characteristics.

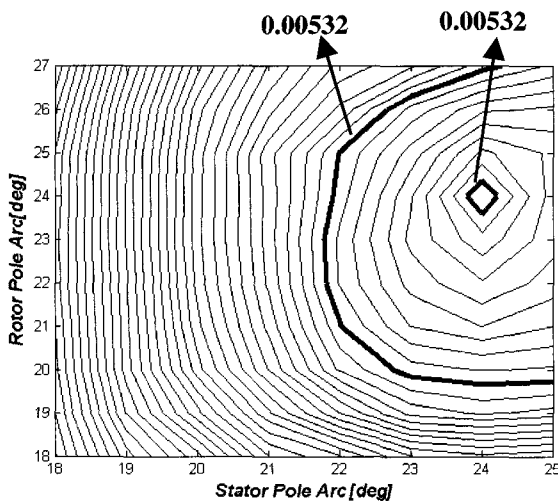


Fig. 4 Contour graph of  $dL/d\theta$  according to pole arcs

Table 2  $dL/d\theta$  according to pole arcs

| $\beta_R \backslash \beta_s$ | 18       | 19       | 20       | 21       |
|------------------------------|----------|----------|----------|----------|
| 18                           | 0.004070 | 0.004277 | 0.004405 | 0.004572 |
| 19                           | 0.004103 | 0.004357 | 0.004532 | 0.004692 |
| 20                           | 0.004126 | 0.004402 | 0.004622 | 0.004792 |
| 21                           | 0.004137 | 0.004407 | 0.004657 | 0.004832 |
| 22                           | 0.004148 | 0.004412 | 0.004678 | 0.004860 |
| 23                           | 0.004151 | 0.004421 | 0.004688 | 0.004869 |
| 24                           | 0.004142 | 0.004419 | 0.004685 | 0.004867 |
| 25                           | 0.004139 | 0.004416 | 0.004681 | 0.004873 |
| 26                           | 0.004097 | 0.004395 | 0.004655 | 0.004813 |
| 27                           | 0.004043 | 0.004340 | 0.004593 | 0.004761 |

| $\beta_R \backslash \beta_s$ | 22       | 23       | 24       | 25       |
|------------------------------|----------|----------|----------|----------|
| 18                           | 0.004633 | 0.004728 | 0.004753 | 0.004737 |
| 19                           | 0.004823 | 0.004928 | 0.004953 | 0.004937 |
| 20                           | 0.004953 | 0.005028 | 0.005043 | 0.005037 |
| 21                           | 0.005007 | 0.005104 | 0.005135 | 0.005104 |
| 22                           | 0.005045 | 0.005147 | 0.005195 | 0.005151 |
| 23                           | 0.005050 | 0.005175 | 0.005249 | 0.005177 |
| 24                           | 0.005025 | 0.005162 | 0.005322 | 0.005182 |
| 25                           | 0.005012 | 0.005117 | 0.005236 | 0.005190 |
| 26                           | 0.004924 | 0.005053 | 0.005128 | 0.005141 |
| 27                           | 0.004864 | 0.004909 | 0.004995 | 0.005049 |

As well, even though the minimum value of the inductance is smaller, the models that have a small stator pole arc have a short inductance rising region where positive torque is generated as well as a maximum inductance region. Due to these reasons, it is possible to predict a degradation of the performance compared to the models whose rotor and stator pole arcs are the same. Thus, concerning the model having identical pole arc for both the stator and the rotor, to satisfy the required  $dL/d\theta$ , the current of the pole is set to 9.92 and through the analysis of inductance the number of turns are decided. The result is indicated in Table 3. The optimal pole arc that satisfies the given conditions of this paper is selected through a process of comparing the performance of each of the models.

Table 3 Turn number and  $dL/d\theta$  of each model.

| Model                         | Turn No. | Resistance | $dL/d\theta$ |
|-------------------------------|----------|------------|--------------|
| $(\beta_s, \beta_R = 18, 18)$ | 44       | 0.198239   | 0.005025     |
| $(\beta_s, \beta_R = 19, 19)$ | 41       | 0.177743   | 0.004973     |
| $(\beta_s, \beta_R = 20, 20)$ | 40       | 0.174791   | 0.005076     |
| $(\beta_s, \beta_R = 21, 21)$ | 38       | 0.163073   | 0.004962     |
| $(\beta_s, \beta_R = 22, 22)$ | 37       | 0.159917   | 0.005045     |
| $(\beta_s, \beta_R = 23, 23)$ | 36       | 0.156693   | 0.005008     |
| $(\beta_s, \beta_R = 25, 25)$ | 35       | 0.158991   | 0.0049       |

### 3.3 Performance comparison of determined models

The waveforms of the current and the torque when the turn-on angle is set as -2, 0 and 2 for the models that have an identical pole arc for both stator and rotor, which is  $(\beta_S, \beta_R = 18, 18)$ ,  $(\beta_S, \beta_R = 19, 19)$ ,  $(\beta_S, \beta_R = 20, 20)$ ,  $(\beta_S, \beta_R = 22, 22)$ ,  $(\beta_S, \beta_R = 25, 25)$  is shown in Fig. 5 and the characteristics of each of the models are shown in Table 4. From the current waveform of Fig. 5, as the pole arc of the stator and rotor decreases, the motional EMF becomes larger than the induced voltage. This results in the angle in which the current begins to drop to increase and consequently the peak amplitude of the current and the torque increases. The increase of the current can be a cause of the heat and also can increase the torque. However, it is not used as an evaluation of the performance. In this paper, as a performance evaluation factor, the ratio of the current against the torque is used.

To see the characteristics of each of the models, referring to Table 4, at the sample region, of the inductance which is 5 degrees to 25 degrees, the average current of the motor (the average current flowing through the 3 poles) is increasing from 30[A] as the pole arcs become smaller. Also, the average torque is larger than 0.8[Nm], which leads to the conclusion that, except

the  $(\beta_S, \beta_R = 25, 25)$  model, the selected models satisfy the initial design factor, which is 9.9243[A] current with a 0.738[Nm](=0.246×3) torque. The average current of the entire interval is about 16[A], and the average torque of the entire region is above 0.25[Nm], which is an acceptable output, except for the  $(\beta_S, \beta_R = 25, 25)$  model. The  $(\beta_S, \beta_R = 19, 19)$  model has the best current to torque ratio performance among the models. In addition, the drive control of the SRM is performed by controlling the turn-on angle depending on the load that will control the generated torque. Fig. 5 shows the characteristics of the following cases; when the turn-on angle has a 2 degree delay with a light load, when the turn-on angle is 0 with the rated load, and when the turn-on angle is shifted -2 degrees earlier with a heavy load. When the turn-on angle is 2 degrees, the average torque is about 0.2[Nm] at a 13[A] average current. This can be compared to the case, when the turn-on angle is -2 degrees. When the turn-on angle is -2 degrees, the average torque is about 0.35[Nm] at a 20[A] average current.

Fig. 6 shows the ratio of current to torque for each pole arc of the stator and rotor. According to the Fig.s, the best model to satisfy the required performance of this paper is the  $(\beta_S, \beta_R = 19, 19)$  model that displays a different result for different rated speeds.

**Table 4** The performance comparison of each model.

(a) -2°

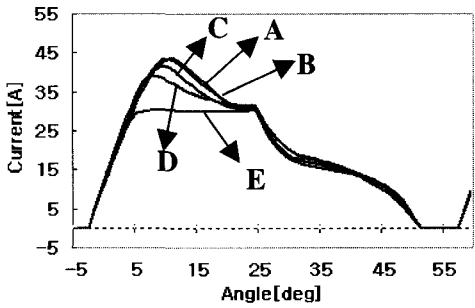
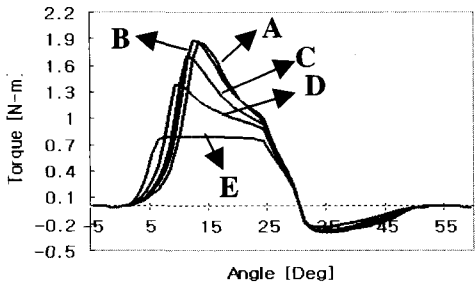
| Item                             | $(\beta_S, \beta_R = 18, 18)$ | $(\beta_S, \beta_R = 19, 19)$ | $(\beta_S, \beta_R = 20, 20)$ | $(\beta_S, \beta_R = 22, 22)$ | $(\beta_S, \beta_R = 25, 25)$ |
|----------------------------------|-------------------------------|-------------------------------|-------------------------------|-------------------------------|-------------------------------|
| Average Current(5°~25°)          | 36.4576                       | 36.626                        | 35.1346                       | 34.414                        | 30.1084                       |
| Average Torque(5°~25°)           | 1.1468                        | 1.2037                        | 1.12479                       | 1.0353                        | 0.7764                        |
| Average Current(0°~60°)          | 20.4965                       | 20.847                        | 20.2987                       | 20.4965                       | 18.6                          |
| Average Torque(0°~60°)           | 0.3517                        | 0.3715                        | 0.3494                        | 0.3256                        | 0.25645                       |
| Average Torque / Average Current | 0.01716                       | 0.01782                       | 0.0172                        | 0.01589                       | 0.0138                        |

(a) 0°

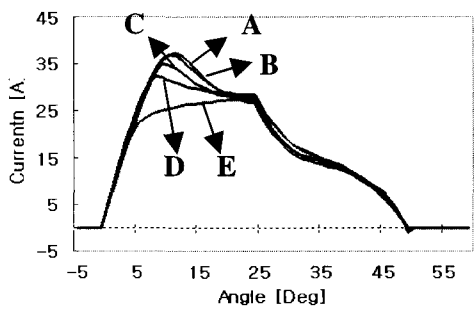
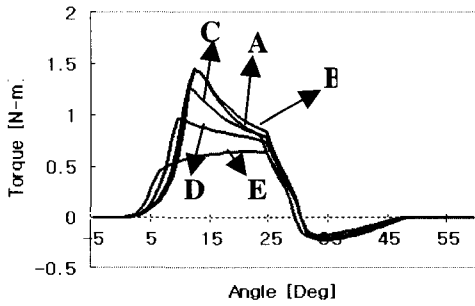
| Item                             | $(\beta_S, \beta_R = 18, 18)$ | $(\beta_S, \beta_R = 19, 19)$ | $(\beta_S, \beta_R = 20, 20)$ | $(\beta_S, \beta_R = 22, 22)$ | $(\beta_S, \beta_R = 25, 25)$ |
|----------------------------------|-------------------------------|-------------------------------|-------------------------------|-------------------------------|-------------------------------|
| Average Current(5°~25°)          | 31.11796                      | 31.3313                       | 30.14825                      | 29.6664                       | 26.25                         |
| Average Torque(5°~25°)           | 0.8747                        | 0.9226                        | 0.8574                        | 0.7822                        | 0.594                         |
| Average Current(0°~60°)          | 16.5476                       | 16.8548                       | 16.4387                       | 16.6                          | 15.17                         |
| Average Torque(0°~60°)           | 0.276                         | 0.2921                        | 0.2725                        | 0.2507                        | 0.197                         |
| Average Torque / Average Current | 0.01668                       | 0.017332                      | 0.016577                      | 0.0151                        | 0.01299                       |

(a) 2°

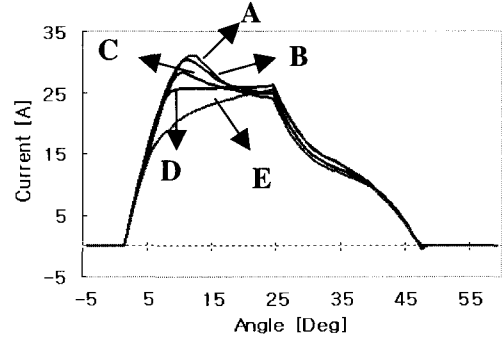
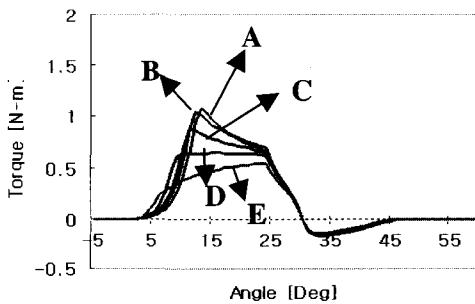
| Item                             | $(\beta_S, \beta_R = 18, 18)$ | $(\beta_S, \beta_R = 19, 19)$ | $(\beta_S, \beta_R = 20, 20)$ | $(\beta_S, \beta_R = 22, 22)$ | $(\beta_S, \beta_R = 25, 25)$ |
|----------------------------------|-------------------------------|-------------------------------|-------------------------------|-------------------------------|-------------------------------|
| Average Current(5°~25°)          | 28.2874                       | 26.4872                       | 25.589                        | 25.35                         | 22.63                         |
| Average Torque(5°~25°)           | 0.66                          | 0.6911                        | 0.6403                        | 0.5821                        | 0.446                         |
| Average Current(0°~60°)          | 13.247                        | 13.4965                       | 13.195                        | 13.391                        | 12.305                        |
| Average Torque(0°~60°)           | 0.2138                        | 0.224                         | 0.208                         | 0.1897                        | 0.1484                        |
| Average Torque / Average Current | 0.016143                      | 0.0166                        | 0.01576                       | 0.01417                       | 0.01206                       |



(a) -2° Turn On, 55° Turn Off



(b) 0° Turn On, 55° Turn Off



(c) 2° Turn On, 55° Turn Off

A : ( $\beta_S, \beta_R = 18, 18$ ), B : ( $\beta_S, \beta_R = 19, 19$ ),  
 C : ( $\beta_S, \beta_R = 20, 20$ ),  
 D : ( $\beta_S, \beta_R = 22, 22$ ), E : ( $\beta_S, \beta_R = 25, 25$ )

Fig. 5 Current and torque waveform of each model

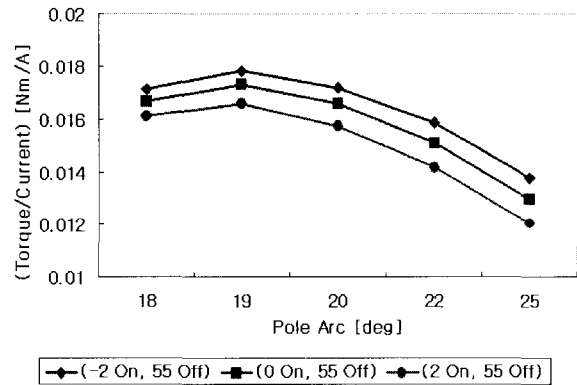


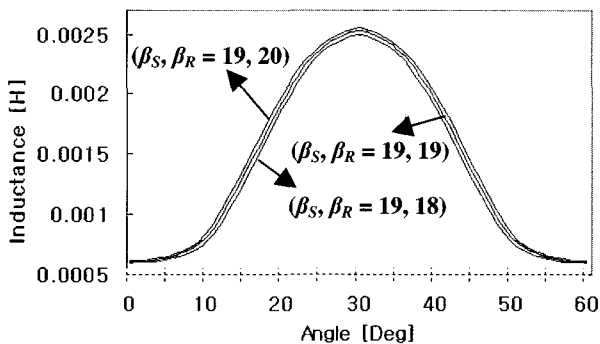
Fig. 6 (Torque/Current) ratio of each model according to the turn on angles

Next, the performance will be compared between the models that have an identical pole arc for the rotor and stator with the models that have a different pole arc. This will be done by some example models, ( $\beta_S, \beta_R = 19, 18$ ), ( $\beta_S, \beta_R = 19, 20$ ) and ( $\beta_S, \beta_R = 19, 19$ ). As the pole arc of the rotor of the three models is identical, it can be said that the slot area and the specifications of the windings are equivalent, which means that there are no differences with the properties of the resistor and iron losses.

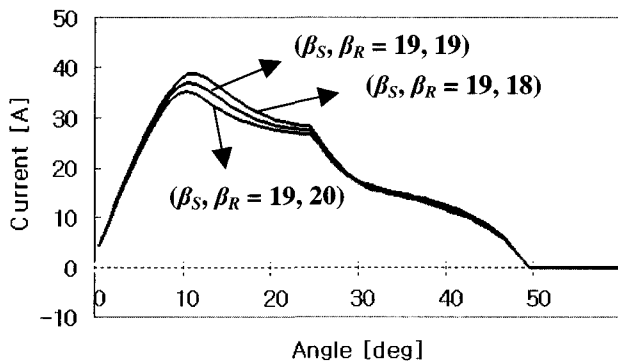
The inductance profiles of the three models are shown in Fig. 7, and for a comparison of the performance, a nonlinear FE analysis was carried out under the condition of a rated voltage of 190[V] and a 0 degree turn-on angle, 25 degree turn-off angle.

Fig. 8 depicts the torque and current waveforms of each of the models and Table 5 shows the characteristics of the models ( $\beta_S, \beta_R = 19, 20$ ) shows a small torque due to the

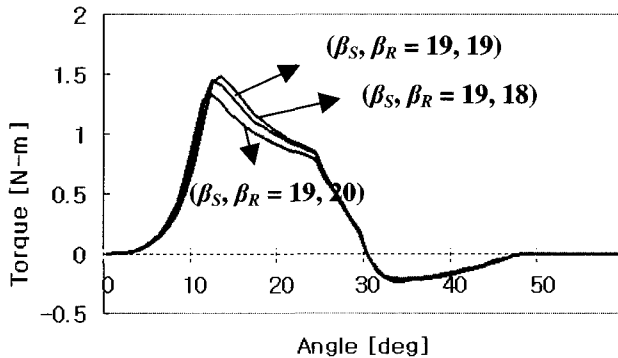
inefficient current, while  $(\beta_S, \beta_R = 19, 18)$  shows the largest current and torque. Considering the ratio of the current to torque, however, the  $(\beta_S, \beta_R = 19, 19)$  model is suitable for the specifications of this paper, which aims for a high speed SRM drive. The experimental proof was impossible for the model that is selected in this paper, because there is no torque-meter that can detect the torque of a high speed motor (above 30,000[RPM]). However, the design procedure that was proposed in this paper, which is the



**Fig. 7** Inductance profiles of  $(\beta_S, \beta_R = 19, 18)$ ,  $(\beta_S, \beta_R = 19, 19)$  and  $(\beta_S, \beta_R = 19, 20)$



(a) Current waveform



(b) Torque waveform

**Fig. 8** Current and torque waveform of  $(\beta_S, \beta_R = 19, 18)$ ,  $(\beta_S, \beta_R = 19, 19)$  and  $(\beta_S, \beta_R = 19, 20)$

**Table 5** Performance comparison of  $(\beta_S, \beta_R = 19, 18)$ ,  $(\beta_S, \beta_R = 19, 19)$  and  $(\beta_S, \beta_R = 19, 20)$

| Item  | $(\beta_S, \beta_R = 19, 18)$ | $(\beta_S, \beta_R = 19, 19)$ | $(\beta_S, \beta_R = 19, 20)$ |
|---|-------------------------------|-------------------------------|-------------------------------|
| Average Current ( $5^\circ \sim 25^\circ$ ) | 32.6976                       | 31.33                         | 30.02                         |
| Average Torque ( $5^\circ \sim 25^\circ$ )  | 0.9267                        | 0.92267                       | 0.871654                      |
| Average Current ( $0^\circ \sim 60^\circ$ ) | 17.48                         | 16.871                        | 16.288                        |
| Average Torque ( $0^\circ \sim 60^\circ$ )  | 0.2927                        | 0.2921                        | 0.2765                        |
| Average Torque / Average Current            | 0.016745                      | 0.017315                      | 0.16976                       |

design flow by selecting the current and  $dL/d\theta$  as an initial design factor, can be thought as an acceptable method judging from the design results.

#### 4. Conclusion

This paper proposed a new design method for a high speed SRM and the design results are shown with their characteristics. The torque characteristics differ mainly by the combinations of the arc angle pole arc of the stator and rotor and the switching conditions such as on and off. FE analysis, which considers the nonlinearity of the magnetic field and the drive circuit, was used for the analysis of the performance, because the SRM are mainly driven under the saturated region with a drive circuit. A summary of the design procedure that this paper proposes is as follows. The initial conditions such as the current and the  $dL/d\theta$  “ $dL/d\theta$ ” are selected first, and based on these conditions the outlines of the motor are specified. By a detailed step of analysis a detailed form of a motor is made. In this paper, the proposed method was proved to be appropriate by inspecting the design results. The design method that was proposed in this paper could be used as an effective method to reduce the trial and errors in case of designing not only a single phase SRM but also a three phase SRM.

#### Acknowledgements

This work was supported by a grant from Hanbat University Academy in 2004.

#### References

- [1] “Technical Trend of Switched Reluctance Motor”, *The Korea n Institute of Electrical Engineers*, 1994,

Special Survey Committee for Reluctance Motor

- [2] J. H. Choi, S. Kim, K. J. Lee, J. Lee, G. J. Hong, D. H. Choi, "Optimization of geometric parameter and electrical parameter for reducing the torque ripple of Switched Reluctance Motor", *The Transaction of the Korea n Institute of Electrical Engineers*, Vol 53, No. 2, pp. 93-100, 2003
- [3] J. H. Moon, S. K. Oh,, J. W. Ahn, "An Analysis of Noise Characteristics According to the Excitation Method of SRM", *The Transaction of the Korea n Institute of Electrical Engineers*, Vol 49, No. 9, pp. 565-571, 2000
- [4] Higuchi, T, Fiedler, J.O, De Doncker, R.W., "On the Design of a single switched reluctance motor," *Electric Machines and Drive Conference, IEMDC'03. IEEE International.*, 2003v.1, pp. 561-567, 2003.
- [5] Krishnan, R., Staley, A.M, Sitapati, K., "A novel single-phase switched reluctance motor drive system," *Industrial Electronics Society, 2001. IECON '01. The 27th Annual Conference of the IEEE*, 2001v.2, pp.1488-1493, 2001.
- [6] J.Y Lim, Y.C Jung, S.Y Kim, J.C Kim, "Single phase switched reluctance motor for vacuum cleaner," *IEEE International Symposium on Industrial Electronics*, 2001. , v.2, pp.1393-1400, 2001. June
- [7] P.J.Lawrenson. J.M.Stephenson, P.T.Blenkinsop, J. Corda and N.N.Fulton, "Variable Speed Switched Reluctance Motor", *Proc. IEE.* pt.B, vol.127, July 1980, pp. 253-265



### Youn-Hyun Kim

He was born in Korea in 1964. He received his B.S., M.S. and Ph.D. degrees in Electrical Engineering from Hanyang University in 1987, 1989 and 2002, respectively. He worked for LG Industrial System Co.,Ltd as a Senior Research Engineer from 1989 to 1999.

Currently, he is a Professor in the Department of Electrical Engineering, Hanbat National University. His research interests are Motor Drive, Design and Analysis of Machines, and Power Electronics.